Diagnosis of turbulence radiation interaction in turbulent flames and implications for modeling in large Eddy simulation

Damien Poitou, Mouna El-Hafi, Bénédicte Cuenot

Diagnosis of Turbulence Radiation Interaction in Turbulent Flames and Implications for Modeling in Large Eddy Simulation

Damien POITOU, Mouna EL HAFI
RAPSODEE research centre - UMR EMAC-CNRS 2392 Ecole des Mines d'Albi Carmaux - Campus Jarlard-81013 Albi Cedex 9, FRANCE
e-mail: poitou@enstimac.fr
Benedicte CUENOT
CERFACS - 42, Avenue Gaspard Coriolis - 31057 Toulouse Cedex 01, FRANCE

Abstract

An *a priori* study of the turbulence radiation interaction (TRI) is performed on numerical data from Direct Numerical Simulation (DNS) of a turbulent flame. The influence of the various correlations that appear in the radiative emission is investigated and their impact is evaluated in the context of Large Eddy Simulation (LES). In LES, only filtered quantities are computed, where the filter is the grid. The radiative emission is reconstructed first from the exact, then filtered solution variables and the sensitivity to the filter size is evaluated. Three approaches are used to take into account the subgrid scale correlations: the no-TRI, partial TRI and full TRI approaches. Results show that the full TRI is exact compared to the reference emission and that the partial TRI performs worse than the no-TRI for the studied configuration. This indicates that in the studied case, the TRI must be considered in LES in a full formulation.

Key words: Turbulence-Radiation Interaction, Large Eddy Simulation, turbulent combustion, radiative transfer.

Introduction

Turbulence is one of the most common state of fluid flows, either in industrial applications or natural phenomena. They develop for example when the Reynolds number $Re{=}UL/\nu$ (where U is the characteristic flow velocity, L is a flow characteristic length and ν is the viscosity), reaches sufficiently high values. Although the general equations of fluid dynamics allow to describe both turbulent and laminar flows, computational constraints limit their resolution and different approaches may be used. Direct numerical simulation (DNS) reproduces exactly the turbulent flow but due to a high CPU cost it is restricted to simple geometries and moderate *Re*. On the contrary Reynolds-Average-Navier-Stokes (RANS) simulations are very fast and handle complex high *Re* flows, but compute only mean solutions of steady flows. The introduction of Large Eddy Simulations (LES) gives access to filtered variables in high *Re*, non stationary complex turbulent flows. However it still requires modeling for the subgrid scale phenomena. In all these simulations the radiative transfer is often omitted because of its complexity and prohibitive calculation time. Nevertheless the concerns about energy savings and environment safeguarding impose significant increase of efficiency and decrease of pollutant emissions. As the production of polluting species, like nitrogen oxide (NO_x) and soot, is known to be very sensitive to temperature levels, radiation has now become a key point in modern combustion simulations.

The importance of turbulence-radiation interaction (TRI) is by now well recognized in the scientific community (Coelho, 2007). This observation is supported by experimental studies, conducted mostly by Faeth and Gore and theirs co-workers over the last

twenty years for a number of fuels (Gore and Faeth, 1988; Kounalakis et al., 1989; Gore et al., 1987a). This experimental data demonstrate that, depending on the fuel, the radiative emission of a turbulent flame may be up to 50 to 300% higher than it would be evaluated from the mean values of temperature and absorption coefficient.

Theoretical studies provide an additional support for the importance of TRI in combustion applications. Cox (1977) shows that the temperature fluctuations may increase the radiative emission by 100% if the level of fluctuation exceeds 41%. He also suggests that the turbulent fluctuations may affect the absorption coefficient leading to an increase of flame emission. Kabashnikov and Myasnikova (1985) formalized the optically thin eddy approximation (OTFA) commonly used for closure models in TRI. They conclude that TRI may increase the radiative intensity by a factor two or three.

In addition, numerous numerical studies have been carried out to demonstrate the effects of TRI and to evaluate the impact of different parameters (Burns, 1999). In uncoupled calculations, the radiative transfer is computed from the temperature and species concentrations provided by experiment or combustion simulation results. The fluctuations are commonly generated by stochastic models. Predictions using stochastic models give results in good agreement with experimental data. With this approach Grosshandler et al. (Grosshandler and Joulain, 1986; Ficher et al. 1987) shows that TRI may increase the radiative intensity by a factor two. In the case of very sooty flames the emission may decrease because of the negative cross-correlation between soot volumetric fraction and temperature. Jeng et al. points out that TRI is weak in carbon monoxide/air flames (in order of 10%) (Gore et al., 1987b), moderate in methane/air flames (in order of 10% to 30%) (Jeng and Lai, 1984) and important in hydrogen/air flames (in order of 100%) (Gore et al., 1987a). Kounalakis, Faeth, Sivathanu, Zheng (Zheng et al., 2002, 2003) or Coelho (2004) also give results in agreement with an increase of radiative emission by TRI. Coupled calculations show that TRI contributes to lower the flame temperature and increase the wall fluxes. Adams and Smith (2003) report temperature reductions by 50K to 100K. These results are confirmed by the work of Li and Modest (2003) also showing that wall fluxes may increase by 40%. Coelho et al. (2003) find that the radiative heat loss may increase by 50% if taking into account all TRI effects.

DNS is a powerful tool to diagnose different effects of TRI and to test usual approximations like the OTFA. It was used recently by Wu et al. (2005) to study TRI in the context of RANS, to evaluate the effect of the deviation from the mean of the solution variables. In LES, only the subgrid part of the fluctuations is unknown and it is a deviation from the local filtered value. Therefore the impact of TRI might be very different and it is the purpose of the present work to analyze it using the same methodology: the radiation calculations are performed as a post-processing treatment of available DNS results (Jiménez and Cuenot, 2007), i.e. in an uncoupled approach. In the following, section 1 gives the basic theoretical elements of the analysis, section 2 describes the configuration and the radiation calculations, and finally section 3 presents the results.

Turbulence Radiation Interaction

LES of turbulent flows

Turbulence is a complex phenomenon involving nonlinear processes and developing over a wide range of spatial and temporal scales. In industrial applications it is characterized by the Reynolds number introduced above and some particular length scales such as the integral length scale l_e corresponding to the largest flow structures or the Kolmogorov scale η associated to the smallest eddies. In the LES description of turbulence, a low-pass filter is used to decompose turbulent quantities into two parts:

$$X = \overline{X} + X' \tag{1}$$

where $\overline{X}$ is the filtered value and X' is the fluctuation. The filtered value is obtained by applying a spatial filter H (Poinsot and Veynante, 2001):

$$\overline{X}(x) = \int_D H(x - x')X(x)dx' \tag{2}$$

where x is the spatial location vector. The filter is characterized by a size Δ. In practice the filter is the grid itself and Δ is directly linked to the mesh size. Note that in general $\overline{X} \neq \overline{X}$ and $\overline{X'} \neq 0$. The relations that are true in the case of a cut-off filter in the spectral space are $\overline{X} = \overline{X}$ and $\overline{X'} = 0$. However, as will be seen later, they are usually assumed to allow model derivations, but it will be also shown that the induced error is weak.

Radiative transfer

In a non-scattering medium, the differential form of the radiative transfer equation is (Modest, 1993; Siegel and Howell, 2002):

$$\frac{\partial I_\nu}{\partial t} + \frac{\partial I_\nu}{\partial s} = \kappa_\nu \left(I_{b\nu} - I_\nu \right) \tag{3}$$

with I_ν the radiative intensity, $I_{b\nu}$ the blackbody radiation intensity, κ_ν the spectral absorption coefficient and s the coordinate along the line of sight.

Spectral model

To take into account the spectral dependence of the radiative properties, several approaches are possible, listed here from the simplest to the highes complexity (and CPU cost): global models (gray gas or weighted sum of gray gases), narrow bands models and finally line-by-line models. In the context of combustion applications, obviously line-by-line models are the most accurate but they have a prohibitive CPU cost. On the other hand global models are not accurate enough in case of non-homogeneous and non-isothermal medium. In a combustion chamber the radiant species being able to contribute to the radiation are H_2O, CO_2 and should be included.

Therefore the Malkmus model using narrow bands represents the best compromise between accuracy and rapidity in this context. The average transmitivity for a narrow band $\Delta\nu$ of a gas thickness layer l is expressed as:

$$\langle \tau \rangle_{\Delta\nu} (l) = \exp \left[\Phi \left(1 + \left(1 + \frac{\langle \kappa \rangle_{\Delta\nu}}{\Phi} \right)^{1/2} \right) \right] \tag{4}$$

where $\langle \kappa \rangle_{\Delta\nu}$ is the average value of the absorption coefficient over the narrow band, and Φ is the shape parameter.

Data for $(\langle \kappa \rangle_{\Delta\nu}, \Phi)$ were taken from the spectroscopic database of Taine and Soufiani (Soufiani and Taine, 1997), that gives values for temperatures between 300K and 2900K and for 367 bands of widths $\Delta\nu$=25 cm. In order to take into account the mixture composition several models are proposed by Liu et al. (2001). The one chosen has the main advantage to insure a good compromise between accuracy CPU time and is based on the optically thin limit, it provide $\langle \kappa_{mix} \rangle$ and Φ_{mix} for a mixture of N_{gas} of parameters κ_n and Φ_n:

$$\langle \kappa_{mix} \rangle_{\Delta\nu} = \sum_{n=1}^{N_{gas}} \langle \kappa_n \rangle_{\Delta\nu} \tag{5}$$

$$\frac{\langle \kappa_{mix} \rangle_{\Delta\nu}^2}{\Phi_{mix}} = \sum_{n=1}^{N_{gas}} \frac{\langle \kappa_n \rangle_{\Delta\nu}^2}{\Phi_n} \tag{6}$$

The spectral dependence of κ is reconstructed from the above average quantities by the k-distribution method that consists in using a distribution function of the absorption coefficients $f(\kappa)$ (Joseph, 2004). The average transmitivity on a narrow band is written as:

$$\langle \tau \rangle_{\Delta\nu} (l) = \int_0^\infty \exp(-\kappa l) f(\kappa) d\kappa \tag{7}$$

It is possible to determine $f(\kappa)$ by observing that $\langle \tau \rangle_{\Delta\nu}$ is the Laplace transform of f:

$$f(\kappa) = T.L.^{-1} \left(\langle \tau \rangle_{\Delta\nu} (l) \right) \tag{8}$$

In general $f(\kappa)$ is not monotonous and two different values of κ may correspond to the same value of f. It is more convenient to introduce the cumulative sum of the probability density function:

$$g(\kappa) = \int_0^\kappa f(\kappa') d\kappa' \tag{9}$$

This function is now bijective and defined in the interval [0,1], which makes it easy to inverse.

In addition for non-homogeneous and no-isothermal media it is necessary to use the so-called assumption of correlated-k, stating that the variations of pressure and temperature on the optical paths do not modify the spectrum or only in a uniform way. This approximation could be used in this application.

To inverse the function $g(\kappa)$ a method developed by Lataillade (2001) based on tabulated values and linear interpolations is used. In this method the coefficients $h_{(i,j)}$, tabulated as functions of the discretized Φ_i (over N_{quad} points) and for each spectral band j, allow to calculate $\kappa_{mix(i,j)}$ as:

$$\kappa_{mix(i,j)} = h_{(i,j)} \left(\Phi_{mix,i} \right) \langle \kappa_{mix} \rangle_{\Delta\nu_j} \tag{10}$$

Finally, to calculate the Planck absorption coefficient, Eq. (14), the integral over each narrow band is calculated:

$$\begin{aligned} \kappa_P &= \tfrac{\pi}{\sigma T^4} \int_0^\infty \kappa_\nu I_{b\nu} d\nu \\ &= \sum_{i=1}^{N_{quad}} \sum_{j=1}^{N_{band}} w_i \kappa_{mix(i,j)} \langle I_b \rangle_{\Delta\nu_j} \Delta\nu_j \end{aligned} \tag{11}$$

In the above expression, $\langle I_b \rangle_{\Delta\nu_j}$ represents the mean Planck function over the narrow band j of width $\Delta\nu$.

Radiative flux

The divergence of the radiative flux $\boldsymbol{q}$ is written as:

$$\nabla \cdot \vec{q} = \int_0^{+\infty} \kappa_\nu \left(4\pi I_{b\nu} - G_\nu\right) d\nu \tag{12}$$

where $G_\nu = \int_{4\pi} I_\nu d\Omega$ is the direction-integrated incident radiation. By integrating over frequencies, one obtains:

$$\nabla \cdot \vec{q} = 4\sigma\kappa_P T^4 - \int_0^{+\infty} \kappa_\nu G_\nu d\nu \tag{13}$$

with $\int_0^\infty I_{b\nu} d\nu = \sigma T^4/\pi$ (σ being the Stephan constant), and introducing the mean Planck absorption coefficient:

$$\kappa_P = \frac{\int_0^\infty \kappa_\nu I_{b\nu} d\nu}{\int_0^\infty I_{b\nu} d\nu} = \frac{\pi}{\sigma T^4} \int_0^\infty \kappa_\nu I_{b\nu} d\nu \tag{14}$$

Radiative transfer in turbulent flames

To study the radiative transfer and TRI in turbulent flames in the LES context, the filtered form of the radiative source term is investigated. By definition:

$$\overline{\nabla \cdot \vec{q}} = 4\sigma\overline{\kappa_P T^4} - \int_0^{+\infty} \overline{\kappa_\nu G_\nu} d\nu \tag{15}$$

Usually in DNS calculations, the quantity $\kappa_P L$, where L is the length of the domain, is small and the medium is optically thin. In the studied case for example $\kappa_P L = 10m^{-1} \times 3mm = 3 \cdot 10^{-2}$. By considering the optically thin approximation (absorption in the medium is negligible), absorption exchanges occur mainly with the walls so that Eq. (15) reduces to:

$$\overline{\nabla \cdot \vec{q}} = 4\sigma\overline{\kappa_P T^4} - \overline{\kappa_P T_\infty^4} = \nabla \cdot q_E - \nabla \cdot q_A \tag{16}$$

where T_∞ is the wall temperature. This approximation is commonly made in combustion applications, and fairly valid for small-scale non-luminous flames. Finally correlations of fluctuating quantities appear only in the emission term $\nabla \cdot q_E$ and the term $\nabla \cdot q_A$ is not investigated in the following.

The emission part of Eq. (15) reveals a correlation between the absorption coefficient and the fourth power of temperature. Using the decomposition of Eq. (1) for κ_P, one gets:

$$\overline{\kappa_P T^4} = \overline{\kappa_P}\,\overline{T^4} + \overline{\kappa_P'}\,\overline{T^4} \tag{17}$$

where it is supposed that $\overline{\overline{\kappa_P}} = \overline{\kappa_P}$ and $\overline{\overline{T^4}} = \overline{T^4}$. This allows to introduce two terms R_{T^4} and R_{Ib} as:

$$\begin{aligned} \overline{\kappa_P T^4} &= \overline{\kappa_P}\,\overline{T^4}\left(\frac{\overline{T^4}}{\overline{T^4}} + \frac{\overline{\kappa_P'}\,\overline{T^4}}{\overline{\kappa_P}\,\overline{T^4}}\right) \\ &= \overline{\kappa_P}\,\overline{T^4}\left(R_{T^4} + R_{Ib}\right) \end{aligned} \tag{18}$$

These two distinct correlations, R_{T^4} and R_{Ib} indicate respectively the temperature auto-correlation and the cross-correlation between temperature and fluctuations of the absorption coefficient. Introducing now the temperature fluctuations, and assuming that $\overline{\kappa_P'} = \overline{(T^4)'} = 0$, it is possible to develop the two contributions as:

$$R_{T^4} = 1 + \frac{\overline{T'^2}}{\overline{T}^2} + \frac{\overline{T'^3}}{\overline{T}} + \frac{\overline{T'^4}}{\overline{T}^4} \tag{19}$$

$$\begin{aligned} R_{Ib} = {} & 4\frac{\overline{\kappa_P' T'}}{\overline{\kappa_P}\,\overline{T}} + 6\frac{\overline{\kappa_P' T'^2}}{\overline{\kappa_P}\,\overline{T}^2} \\ & + 4\frac{\overline{\kappa_P' T'^3}}{\overline{\kappa_P}\,\overline{T}^3} + \frac{\overline{\kappa_P' T'^4}}{\overline{\kappa_P}\,\overline{T}^4} \end{aligned} \tag{20}$$

Assuming that the intensity of fluctuations is low, correlations of higher order than two may be dropped, leading to as proposed by Snegirev (2004):

$$R_{T^4} \approx 1 + \frac{\overline{T'^2}}{\overline{T}^2} \text{ and } R_{Ib} \approx 4\frac{\overline{\kappa_P' T'}}{\overline{\kappa_P}\,\overline{T}} \tag{21}$$

Assuming that the impact of species concentration fluctuations is negligible on κ_P , this has been checked numerically, a second-order Taylor expansion of $\kappa_P(T) = \kappa_P(T + T')$ is performed:

$$\begin{aligned} \kappa_P(T) = {} & \kappa_P(\overline{T}) + T'\left(\frac{\partial \kappa_P}{\partial T}\right)_{\overline{T}} \\ & + \frac{T'^2}{2}\left(\frac{\partial^2 \kappa_P}{\partial^2 T}\right)_{\overline{T}} + \dots \end{aligned} \tag{22}$$

and after filtering:

$$\overline{\kappa_P}(T) = \overline{\kappa_P}(\overline{T}) + \frac{\overline{T'^2}}{2}\left(\frac{\partial^2 \kappa_P}{\partial^2 T}\right)_{\overline{T}} + \dots \tag{23}$$

Multiplying $\kappa_P - \overline{\kappa_P} = \kappa_P'$ (from Eq .(22) and Eq. (23)), by T' and filtering, one finally obtains (at the second order):

$$R_{Ib} \approx 4\frac{\overline{T'^2}}{\overline{\kappa_P}\,\overline{T}}\left(\frac{\partial^2 \kappa_P}{\partial^2 T}\right)_{\overline{T}} \tag{24}$$

Not surprisingly, the cross-correlation between T and κ_P is expressed through the derivative $\partial\kappa_P/\partial T$.

From this development it is possible to identify three different approaches to describe the TRI process. The most simple is the no-TRI approach, where $R_{T^4} = 1$ and $R_{Ib} = 0$, so where the TRI effects are ignored. In the partial TRI approach only the temperature auto-correlation is considered and $R_{Ib} = 0$, whereas in the full TRI approach both correlations are considered. These three approaches are evaluated and compared in the next sections.

Configuration and Physical Model

DNS calculation

Results of the direct numerical simulation (DNS) of a reactive turbulent flame are used for the TRI analysis. The data were provided by Jiménez (Jiménez and Cuenot, 2007), and reproduced the stabilization of a triple flame by inert hot gas. The flow configuration is a mixing layer of diluted methane (CH_4 20 % , N_2 80 % in volume) and air, as seen on Figure 1. A hot gas layer is set above the air flow to stabilize the flame.

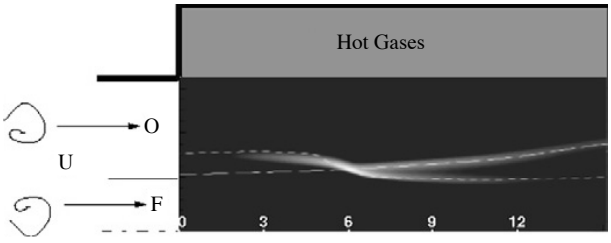

Figure 1. Simulation configuration and initial laminar flame. The rate of reaction is represented in levels of gray where the white represents the maximum. The lines represent the stoichiometric contour (long dash) and isotemperature line $T_i = T_0 + 0.5(T_{ad} + T_0)$ (short dash), where T_0 is the temperature for fresh gases and T_{ad} the adiabatic flame temperature (Jiménez and Cuenot, 2007).

The DNS are run by solving the fully compressible conservation equations for mass, momentum, energy and chemical species in a two dimensional Cartesian domain with a grid of 300 x 200 points, representing a physical space of 3 x 2 mm (Jiménez and Cuenot, 2007).

After the laminar flame is stabilized, turbulence is injected into the domain to obtain a turbulent flame (Figure 2). The hot gas layer allows flame stabilization by the recirculation of hot gas. A zone of recirculation is created in the left higher corner, where the hot gas are trapped, providing the energy necessary to stabilize the flame (shown by the left arrow on Figure 2), that otherwise would be convected downwards and finally blow off. The hot gas produced by combustion are brought back by the recirculation towards the left higher corner to maintain the reserve of energy (right arrow on Figure 2).

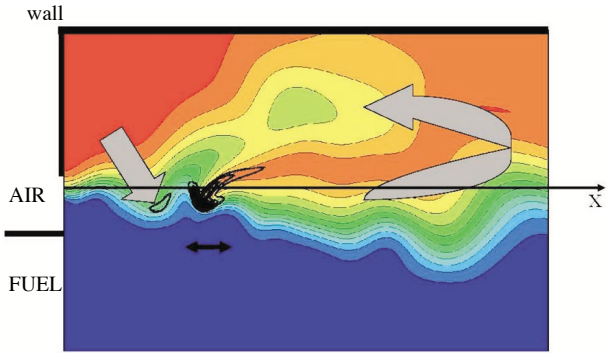

Figure 2. Instantaneous fields of temperature (in levels of gray) and isocontours of rate of reaction (black lines) in the turbulent flame.

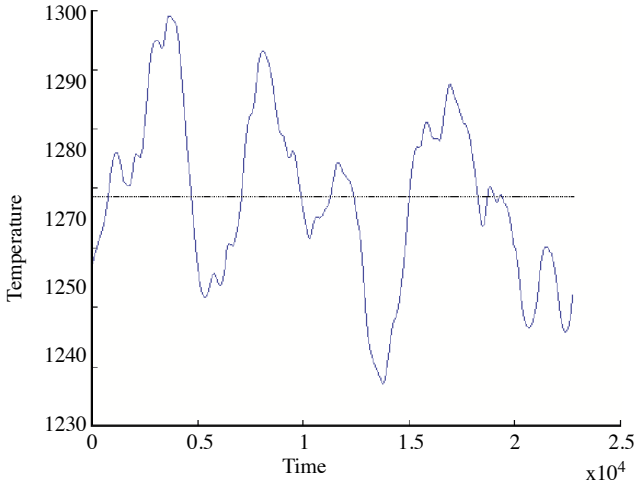

Figure 3. Evolution of the space mean temperature versus time.

After sufficient time the average temperature remains close to constant, and the mean flow may be considered stationary, allowing to collect statistics (Figure 3) .

The available data include density, velocity, total energy, mass fraction of the reactants (fuel and oxidant) as well as the temperature. These two last variables are used in our study to calculate the radiative terms in a post-processing approach.

TRI analysis

This study is performed in two steps. First, a diagnosis allows to evaluate the impact of filtering. Then modeling aspects are considered.

DNS results provide exact data for T and κ_P and give access to the exact emission $\kappa_P T^4$. DNS also allows to compute "exact" filtered quantities ($\overline{T}$,$\overline{\kappa_P}$,$\overline{T^4}$...) and fluctuations (T', κ'_P,...), as well as all types of correlations ($\overline{\kappa'_P T'}$,...). By definition, and supposing all assumptions valid, the full TRI approach should recover the "exact" filtered radiation terms.

In a LES only the filtered values of temperature and species concentrations are available but the filtered value of $\overline{T^4}$ or the correlation $\overline{\kappa'_P T'}$ for example are unknown. Models are therefore needed to reconstruct them and DNS is used to evaluate and validate them.

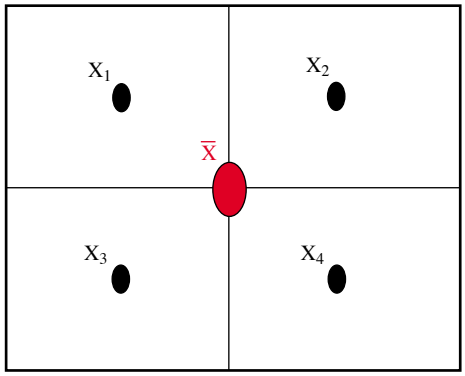

Figure 4. Example of mesh filter.

To reproduce the filter of a LES calculation, a box filter is applied to the DNS data as illustrated in Figure 4. In this example the size of the filter is $2\Delta x$ (Δx being the mesh size of the uniform mesh used in DNS) and the filtered value is obtained by $\overline{X} = (X_1 + X_2 + X_3 + X_4)/4$. More generally the expression of the filtered value at a node (i,j) is:

$$\overline{X_{i,j}} = \frac{1}{N_{filt}^2} \sum_{k=i-N_{filt}/2}^{i+N_{filt}/2} \sum_{l=j-N_{filt}/2}^{j+N_{filt}/2} X_{kl} \qquad (25)$$

where N_{filt}^2 is the number of cells involved and X_{kl} is the exact value from the DNS. The filter size is $N_{filt}\Delta x$. The subgrid fluctuations are then given by the difference between the exact value (from the DNS) and the filtered value:

$$X'_{kl} = X_{kl} - \overline{X_{ij}} \qquad (26)$$

The spatial mean over the whole domain of the intensity of fluctuation is then defined as:

$$X_{RMS} = \left\langle \frac{\sqrt{\overline{X'^2}}}{\overline{X}} \right\rangle \qquad (27)$$

In a first step the analysis was done only along the central axis (in the longitudinal direction) of the configuration, where the fluctuations are most important and to better visualize the effects of filtering. In this case the filter operator is applied in the longitudinal direction only. The analysis of the total emission over the whole domain is made in a second step using a "box" filter as presented previously. Calculations were carried out for various filter sizes going from 1x1 Δx (i.e. no filter) to 100x100 Δx.

Results

Filtered data analysis

If the subgrid fluctuations are homogeneously distributed in the domain, the intensity X_{RMS} first increases with the filter size to reach a constant value after some point. If on the contrary there are important heterogeneities in the fluctuations, the intensity X_{RMS} also starts to increase with the filter size but may either continue to increase or decrease when heterogeneity is reached by the filtering box. In the studied case there are heterogeneities in temperature and species concentrations fluctuations, with important levels in the vicinity of the flame and much lower levels away from the flame. As shown on Figure 5, these homogeneities are sufficient to modify the slope of the curve X_{RMS} versus N_{filt} but not to change its sign that stays always positive up to the maximum size filter.

On Figure 6 the exact emission profile $\nabla \cdot q_{E,DNS}$ is shown along the central axis (see Figure 2) and exhibits strong variations due to the presence of the flame. For comparison purposes, the exact filtered emission $\nabla \cdot q_{E,ref}$ (called the reference emission) as well as the emission resulting from the no-TRI, partial TRI and full TRI approaches are also plotted. As expected the full TRI approach is in exact agreement with the reference, demonstrating the validity of the assumptions made on the filter operator. However what is more surprising is that the no TRI approach , although not as good as the full TRI, is by far much better than the partial TRI approach.

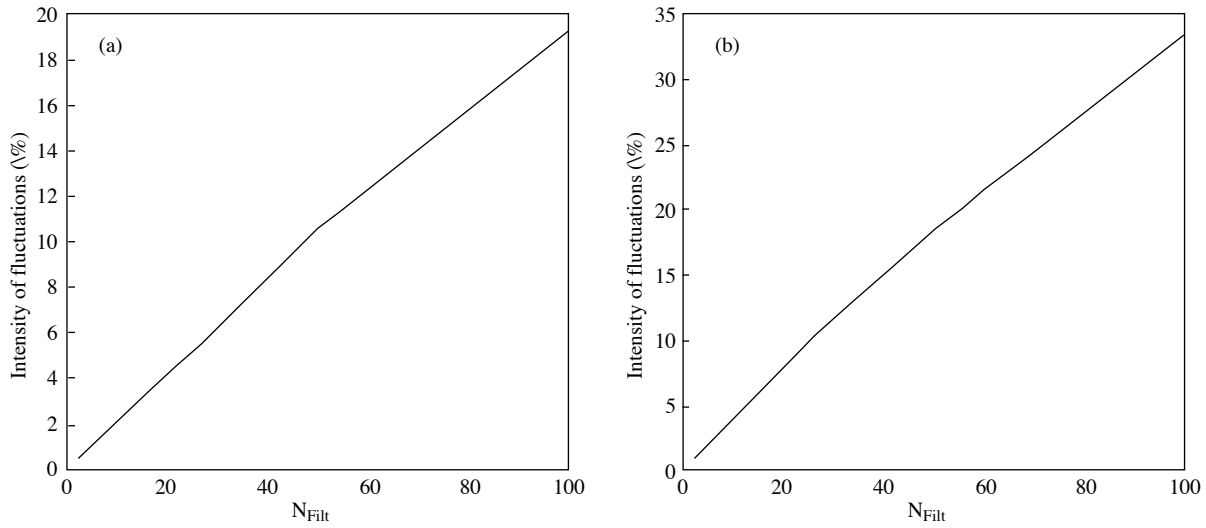

Figure 5. Fluctuation intensity over the whole domain, in percentage, of a. temperature, b. absorption coefficient, versus the filter size.

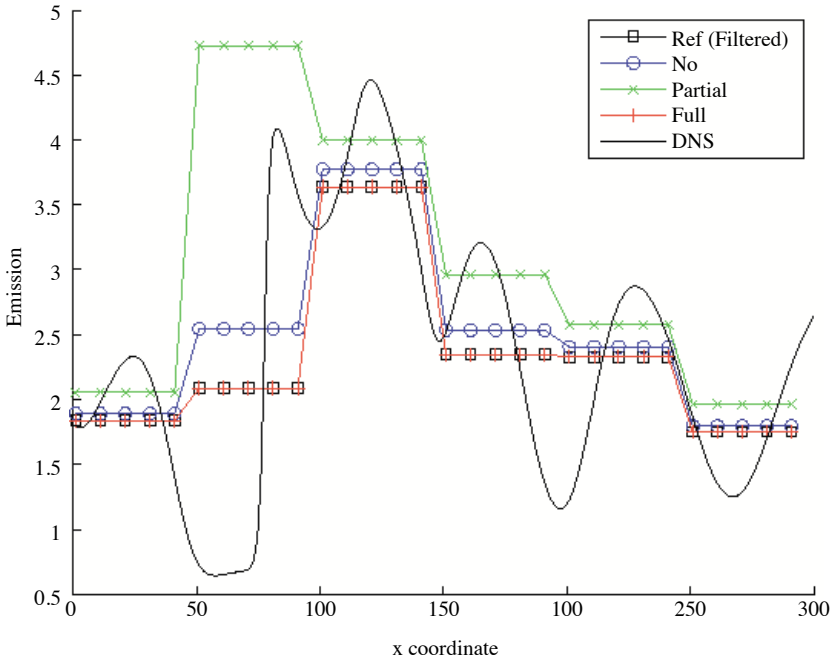

Figure 6. Emission profile along the flame axis for a filter of 50 Δx.

Figure 7a shows the relative error along the flame axis, for different filter sizes, defined as:

$$\varepsilon = \left\langle \left(\frac{\nabla \cdot q_E}{\nabla \cdot q_{E,ref}} - 1 \right) \times 100 \right\rangle \qquad (28)$$

where the mean $\langle\rangle$ is taken along the axis. Also shown is the variance of the deviation from this mean value, represented by a vertical bar. The full TRI approach error is below 10^{-6} and even has a tendency to decrease when the filter size increases. On the contrary the no TRI and partial TRI approaches show errors up to 10% and even higher for the latter. This is due to the sign of the correlation between the temperature and the absorption coefficient, that is negative in all present cases. The two correlations (R_{T^4} and R_{Ib}) have then opposite effects that are of the same order of magnitude and tend to unity. Taking into account only one of them introduces therefore

large errors. In this case TRI should never be taken into account in a partial way but always in a complete way, including all terms of the development.

This result show a reverse trend to the vast majority of the TRI literature, because in this configuration the correlation R_{Ib} is negative, it is usually shown that TRI contribute to increase radiative emission . In the literature this correlation is generally positive for gaseous media, the absorption coefficient depends on both mole fractions of the species and temperature, and the dependence on mole fraction is dominant, except for mixture fraction close to the stoichiometric value (see Figure 6 in Deshmukh et al., 2006). In this configuration fluctuations responsible for TRI are only important along the central axis, this region is closed to stoichiometric values (see Figure 1) so only the temperature contribution on the absorption coefficient is important in a negative way.

The same analysis performed over the whole domain shows similar results and leads to the same conclusions, as seen on Figure 7b where the error curves are very similar to the curves plotted along the flame axis.

Modeling

Taking into account the TRI implies then the reconstruction of both R_{T^4} and R_{Ib}. These correlations are not available in LES and need to be modeled. They may be evaluated from Eq. (19) and Eq. (20), using the filtered temperature $\overline{T}$ and absorption coefficient $\overline{\kappa_P}$, and their subgrid scale fluctuations T' and κ'_P. However LES gives $\overline{T}$ but not T', and several approaches may be used to calculate it, that are largely presented in the literature and are not developed here. For the purpose of the present work, T' is directly reconstructed from the DNS data, as well as κ'_P and the other correlations of Eq. (20). This was done along the central axis for a 100 Δx filter. The relative error found on R_{T^4} and R_{Ib} is null. This is not surprising as Eq.(19) and Eq. (20) are exact expressions of the correlations in the full TRI approach. The difficulty is in the evaluation of the above-mentioned subgrid scale variables, that are unknown in LES. In an attempt to reduce the number of unknown $\kappa'_P - T'$ correlations and high order moments of temperature, terms of higher order than two have been dropped in Eq. (19) and Eq. (20) leading to Eq. (21). This led to an error lying between 0.1% and 1% on R_{T^4}, still acceptable, but between 3% and 6% on R_{Ib}. Then, a first consideration towards LES modeling, Eq. (24) is tested. It requires the calculation of the term $\partial\kappa_P/\partial T$, that was evaluated with a simplified spectral model considering water emission only and the weighted sum of gray gas model. Second order correlations calculated from DNS and model based on a Taylor expansion are shown on Figure 8.

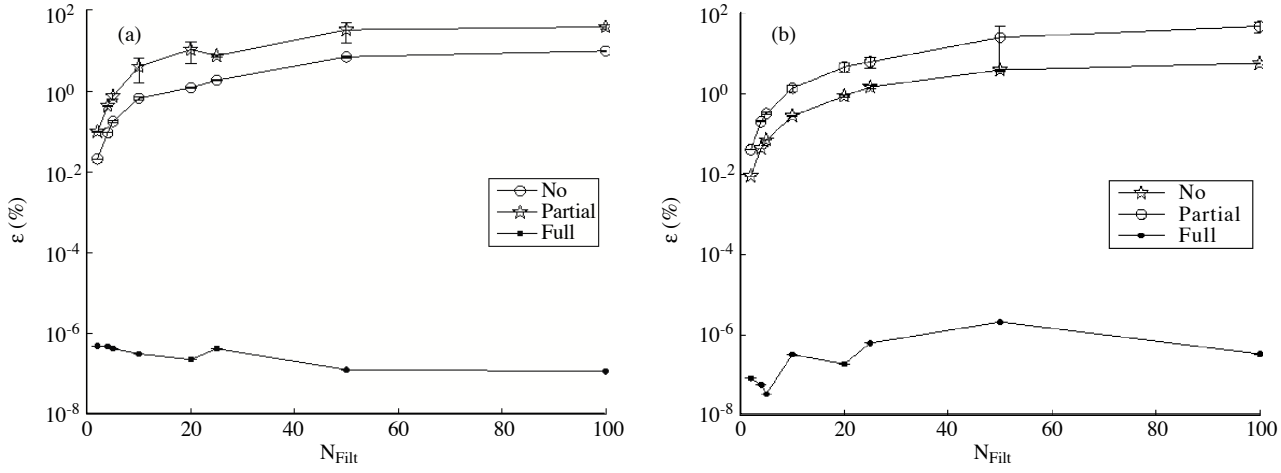

Figure 7. Relative error ε, a. along the axis of the flame, b. over the whole domain, versus the filter size for the various approaches.

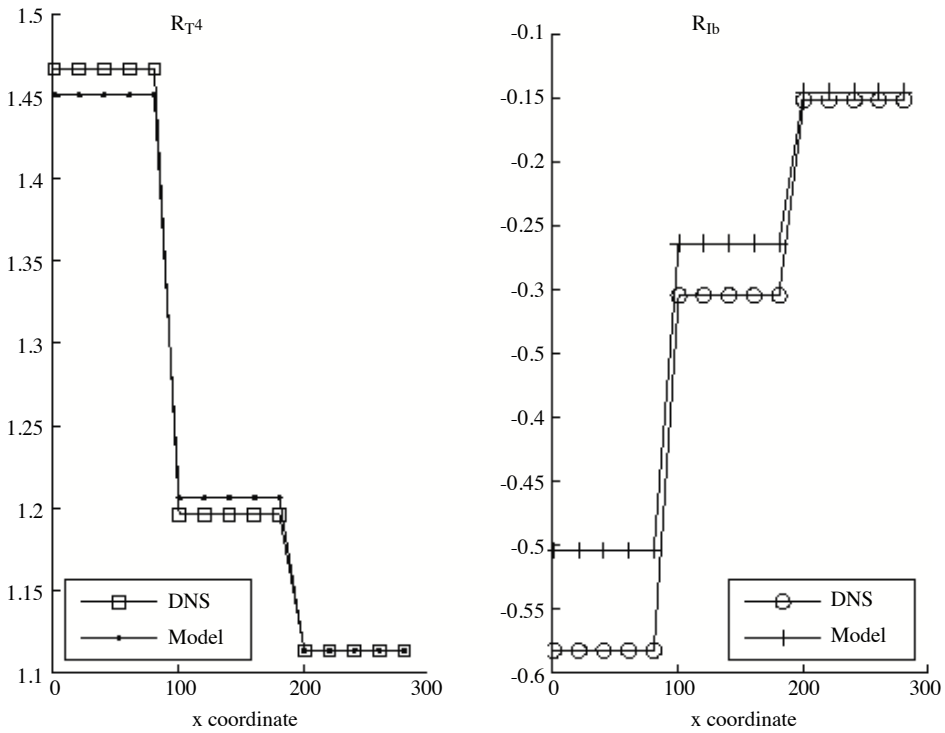

Figure 8. Correlation for R_{T^4} and R_{Ib}, for a filter of 100 Δx along the central axis. Calculated exactly from DNS and modeled by dropping correlation of higher order than two, the Taylor expansion is used to model R_{Ib}.

An important error on R_{Ib} appears for low values of the filter size (29%), due to the fact that the dependence of κ_P with the species was neglected, and for large filter sizes, temperature fluctuations dominate. Adding the species dependency of κ_P allowed to decrease the error to few percents for the low values of the filter size, but increased the error for larger sizes (from 10% to 16%). In this case, the best result is obtained around a filter size of 20 Δx, corresponding to a filtering mesh size of 0.2 mm, which is approximately one order of magnitude smaller than usual LES mesh sizes. This preliminary results give first trends for R_{T^4} and R_{Ib} modeling. Further analysis is needed to better understand the physical mechanisms and improve the models.

Conclusions

An a priori study was conducted from DNS of turbulent flames to characterize the influence of the various correlations that appear in the emission part of the radiative flux in the context of LES. The comparison between the exact and the filtered radiation emission calculated from the DNS and the same quantity calculated from the filtered data showed important discrepancies. Three approaches were defined in taking into account the various correlations in the radiation calculation: the no TRI ignores the correlations, the partial TRI involves the temperature auto-correlation only, and the full TRI adds the temperature/absorption coefficient correlation. As expected the full TRI is exact compared to the reference emission but the partial TRI approach performs worse than the no TRI approach. This shows that in the studied configuration, using only one of the two parts of the subgrid TRI is nonsense and that the full formulation should always be used. The effect of the filter size on the subgrid scale fluctuations is also investigated.

Simple models are evaluated to reconstruct the correlations in a LES framework. Results showed that if the dependency of the absorption coefficient with the species concentrations is included, good predictions may be obtained at small and moderate filter sizes. However all models failed for large filter sizes, in particular for the temperature-absorption coefficient correlation.

One major difficulty that was not addressed in the present paper is to evaluate subgrid scale variances and correlations needed by the radiation calcu-

lation and not directly available in a LES. This will be the next step of the present work, that will be now based on a posteriori analysis of LES calculations in both uncoupled and coupled way.

Nomenclature

Latin

$f(\kappa)$	distribution function of the absorption coefficient
$g(\kappa)$	cumulative sum of the probability density function $f(\kappa)$
G_ν	direction-integrated incident radiation
$H(x)$	filter function
$h_{(i,j)}$	tabulated values of the function $h = g(\kappa)/\langle\kappa_{mix}\rangle$
I_ν	spectral radiation intensity
$I_{b\nu}$	Planck function
l	gas thickness layer
N_{filt}	filter size
N_{gas}	number of species
$\vec{q}$	radiative flux
q_A	absorption term
q_E	emission term
R_{Ib}	cross-correlation between temperature and fluctuations of fluctuations of the absorption coefficient
R_{T^4}	autocorrelation temperature coefficient
Re	Reynold number
s	coordinate along the direction of propagation of a radiation beam
T	temperature
t	time
$T.L.$	Laplace transform
T_∞	wall temperature
w	quadrature weight in the SNB-CK model
x	axial coordinate

Greek

Δx	mesh size
ε	relative error for each approach averaged along the flame axis for a given filter size
κ	abspotion coefficient
κ_n	spectral absorption coefficient over a narrow band $\Delta\nu$ for the n*th gas*
κ_P	mean Planck coefficient
κ_ν	spectral absorption coefficient
$\langle\kappa\rangle_{\Delta\nu}$	spectral absorption coefficient averaged over a narrow band of width $\Delta\nu$
$\langle\kappa_{mix}\rangle$	spectral absorption coefficient averaged over a narrow band of width $\Delta\nu$ for the mixture of species
Ω	solid angle
Φ	shape parameter for the Malkmus model
Φ_n	shape parameter for the Malkmus model for the n*th* gas
Φ_{mix}	shape parameter for the Malkmus model for the mixture of species
σ	Stephan-Boltzmann constant
$\langle\tau\rangle_{\Delta v}$	spectral transmittivity averaged over a narrow band of width $\Delta\nu$

Subscripts and Superscripts

$(\,)_{RMS}$	fluctuation intensity value
ν	wavenumber
i	quadrature point
j	number of spectral band
$(\,)'$	fluctuating componement
$(\bar{\ })$	filtered value

References

B.R. Adams and P.J. Smith, "Modelling of soot and turbulent-radiation coupling on radiative transfer in turbulent gaseous combustion", Comb Sci Technol, 109: 121–140, 2003.

S.P. Burns, "Turbulence radiation interaction modeling in hydrocarbon pool fire simulation", SANDIA Report, SAND99-3190, 1999.

P.J. Coelho, "Detailed numerical simulation of radiative transfer in a non-luminous turbulent jet diffusion flame", Combustion and Flame, 136: 481–492, 2004.

P.J. Coelho, "Numerical simulation of the interaction between turbulence and radiation in reactive flows", Progress in Energy and Combustion Science, 33: 311–383, 2007.

P.J. Coelho, O.J. Teerling, and D Roekaerts, "Spectral radiative effects and turbulence/radiation interaction in a non-luminous turbulent jet diffusion flame", Comb Flame, 133: 75–91, 2003.

G. Cox, "Radiant Heat Transfer in Turbulent Flames", Combustion Science and Technology, 17: 75–78, 1977.

K.V. Deshmukh, M.F. Modest, and D.C Haworth, "Direct numerical simulation of turbulence radiation in a statistically one-dimensional non premixed system", In Lybaert P Lemmonier D, Selçuk N, editor, Proceedings of Eurotherm seminar 78 - computational thermal radiation in participating media II, pages 235–244. Lavoisier, 2006.

S.J. Fisher, B. Hardoiun-Duparc, and W.L. Grosshandler, "The structure and radiation of an ethanol pool fire", Combust Flame, 70: 291–306, 1987.

J.P. Gore and G.M. Faeth, "Structure and Radiation Properties of Luminous Turbulent Acetylene/Air Diffusion Flames", Journal of Heat Transfer, 110: 173–181, 1988.

J.P. Gore, S.M. Jeng, and G.M. Faeth, "Spectral and Total Radiation Properties of Turbulent Hydrogen/Air Diffusion Flames", Journal of Heat Transfer, 109: 165–171, 1987a.

J.P Gore, S.M. Jeng, and G.M. Faeth, "Spectral and Total radiation proprieties of turbulentcarbon monoxyde/air diffusion flames", AIAA J, 25: 339–345, 1987b.

W.L. Grosshandler and P. Joulain, "The effect of large-scale fluctuations on flame radiation", Prog Aeronaut Astronaut, 52(105-123), 1986.

S.M. Jeng and G.M. Faeth M.C. Lai, "Non luminous radiation in turbulent buoyant axisymmetric flames", Combust Sci Technol, 40: 41–53, 1984.

C. Jiménez and B. Cuenot, "DNS study of stabilisation of turbulent triple flames by hot gases", In The Combustion Institute, editor, *Proceedings of the combustion institute*, volume 31(I), pages 1649–1656, 2007.

D. Joseph, "Modelisation des transferts radiatifs en combustion par méthode aux ordonnées discrètes sur des maillages non structurés tridimensionnels", PhD thesis, Institut National Polytechnique de Toulouse, 2004.

V.P. Kabashnikov and G.I. Myasiwkova, "Thermal Radiation in Turbulent Flows - Temperature and Concentration Fluctuations", Heat Transfer - Soviet Research, 17(6): 116–125, 1985.

M.E. Kounalakis, J.P. Gore, and G.M. Faeth, "Mean and fluctuating radiation proprieties of non premixed turbulent carbon monoxide/air flames", Journal of Heat Transfer, 111: 1021–1030, 1989.

A. De Guilhem De Lataillade, "Modélisation détaillée des transferts radiatifs et couplage avec la cinétique chimique dans des système en combustion", PhD thesis, Institut National Polytechnique de Toulouse, 2001.

G. Li and M.F. Modest, "Importance of turbulence radiation interactions in turbulent diffusion jet flames", J Heat Transf, 125: 831–838, 2003.

F. Liu, G.J. Smallwood, and O.L. Gülder, "Application of the statistical narrow-band correlated-k method to no grey gas radiation in mixtures ; Approximate treatment of overlapping bands", J Quant Spectrosc Radiative Transfer, 68: 401–417, 2001.

M.F. Modest, "Radiative Heat Transfert", Mc Graw Hill International Editions, 1993.

T. Poinsot and D. Veynante, "Theorical and Numerical Combustion", Edwards, 2001.

R. Siegel and J.R. Howell, "Thermal Radiation Heat Transfer", Taylor and Francis, 4th edition edition, 2002.

A.Y. Snegriev, "Statisical modelling of thermal radiation transfer in buoyant turbulent diffusion flames", Comb Flame, 136: 51–71, 2004.

A. Soufiani and J. Taine, "High temperature gas radiative propriety parameters of statistical narrow-band model for H_20, CO_2 and CO and correlated-K model for H_20 and CO_2", Technical note in International Journal of Heat and mass transfer, 40: 987–991, 1997.

Y. Wu, D.C. Haworth, M.F. Modest, and B. Cuenot, "Direct numerical simulation of turbulent radiation interaction in premixed combustion systems", Proc Combust Int, 30: 639–646, 2005.

Y. Zheng, Y.R. Sivathanu, and J.P. Gore, "Measurements and stochastic time and space series simulations of spectral radiations intensities for turbulent non-premixed and partially premixed flames", Proc Comb Inst, 29: 1957–1963, 2002.

Y. Zheng, R.S. Barlow, and J.P. Gore, "Spectral radiation proprieties of partially premixed turbulent flames", Journal of Heat Transfer, 125(1065-1073), 2003.